

# Infrared Observations of AR Ursae Majoris: Modeling the Ellipsoidal Variations

Steve B. Howell

Astrophysics Group, Planetary Science Institute  
620 N. 6th Avenue, Tucson, AZ 85705

Dawn M. Gelino & Thomas E. Harrison

Department of Astronomy,  
New Mexico State University, Las Cruces, NM 88003

Submitted to *The Astronomical Journal*

## ABSTRACT

We have obtained time-series infrared photometry for the highly magnetic cataclysmic variable AR UMa. Our J and K' band observations occurred during a low state and they show a distinctive double-humped structure. Using detailed models for the expected ellipsoidal variations in the infrared due to the non-spherical secondary star, we find that the most likely value for the system inclination is  $70^\circ$ . We also model low state V band photometry and find that its observed double-humped structure is *not* caused by ellipsoidal variations, as they have been ascribed to, but are due to beamed cyclotron radiation. We use this result to estimate the magnetic field strength of the active southern accretion region ( $B \lesssim 190$  MG) and its magnetic longitude ( $\psi_S \sim 330^\circ$ ).

*Subject headings:* cataclysmic variables – stars: binaries: close – stars: magnetic – stars: low mass

## 1. Introduction

AR Ursae Majoris is the highest magnetic field strength polar known. Polars, highly magnetic cataclysmic variables (CVs), are interacting binaries which contain a white dwarf primary and a low mass secondary star. The secondary fills its Roche lobe and transfers mass to the gravitational potential of the more massive white dwarf. The white dwarf possesses a strong (usually  $\sim 10\text{--}60$  MG) magnetic field which diverts the transferred material from its ballistic trajectory and funnels it along magnetic flux tubes. This confinement of the accreted material results in the formation of accretion columns which impact the white dwarf at one, or both, of its magnetic poles.

Detailed observational work on AR UMa has been performed by Remillard et al. (1994), Schmidt et al. (1999), Szkody et al. (1999), and references therein. These authors have discussed results of visible, X-ray, and EUV observations of this binary including determinations of an orbital period of 115.9 minutes, a white dwarf mass of  $0.6 \pm 0.2 M_{\odot}$ , and a binary inclination of  $40^{\circ}$  to  $60^{\circ}$ . AR UMa, like all polars, shows modulations in its brightness over periods of weeks to months which is believed to be caused by changes in the rate of mass accretion from the secondary star. The cause of these changes in  $\dot{M}$  are not entirely understood, but may be related to star-spot activity on the secondary (Howell et al. 2000a). During high states, the active accretion region in AR UMa is small in size but very hot ( $\sim 250,000$  K; Szkody et al. 1999; Belle et al. 2000) and located near the south rotation pole of the primary star (co-latitude of  $10^{\circ}\text{--}35^{\circ}$ ). High state observations reveal  $V=15.1$  mag and a dramatic change in EUV and X-ray emission, during which AR UMa becomes the brightest EUV source in the sky. AR UMa, however, spends most of its time in a low state which is characterized by a  $V$  magnitude near 16.5 and weak high energy emission.

Low state  $V$  and  $I$  band photometric observations of AR UMa show a double-humped structure. The cause of these modulations is generally assumed to be ellipsoidal variations (Russell 1945). If true, infrared observations of AR UMa would be expected to be dominated by ellipsoidal modulations and allow detailed modeling of the secondary star. Such data could reveal quantitative measures of the secondary star mass and temperature, as well as place additional constraints on the system parameters. We therefore undertook IR photometric observations of AR UMa in the  $J$  and  $K'$  bands.

In section 2, we describe our observations and data reduction, as well as present our IR photometric light curves. Section 3 describes our optical and infrared light curve modeling procedure using WD98, the newest version of the Wilson-Devinney light curve modeling code. We provide details of how we chose the relevant input parameters and present the resulting models at  $V$ ,  $I$ ,  $J$ , and  $K'$ . Finally, Section 4 discusses the implications of these models.

## 2. Observations & Data Reduction

AR UMa was observed using IRIM (see Joyce 1999) on the Kitt Peak National Observatory 2.1-m telescope on 13 and 14 February 2000. On 13 February, AR UMa was observed from 8:32 to 10:45 UT, and on 14 February from 8:43 to 10:51 UT with each session covering slightly more than one AR UMa orbital period. Photometric data were obtained in the IRIM J ( $\lambda_c=1.25\ \mu\text{m}$ ) and K' ( $\lambda_c=2.15\ \mu\text{m}$ ) filters. Our observing sequence consisted of two J images at one position, a beam switch, then two additional J images. We then switched to the K' filter, refocused, and repeated the procedure. Each individual J image consisted of 4 co-added frames of 10 seconds each, while the corresponding K' images consisted of 10 co-added frames of 4 seconds each.

Both sky flats and dome flats were obtained. Before processing, all of the image data were linearized using the *irlincor* package within IRAF with the coefficients suggested for use in the IRIM User's Manual (Joyce 1999). After averaging the two images at one position, we subtracted them from the average of the two images at the other position. These sky, and bias-subtracted images were then flat fielded using a flat constructed by averaging together a median of the dome and sky flats.

Aperture photometry was performed on AR UMa and two roughly equal brightness nearby field stars (a close optical pair at RA=11:15:42, DEC=+42:55:20) used as comparisons. Using the *phot* package in IRAF, instrumental magnitudes were measured and a differential light curve in both J and K' was generated with each point being the average of the two beam switched images. Mid-exposure times were heliocentric corrected. Proper magnitude uncertainties were determined according to the prescription given by Howell et al. (1988) with the average error being  $0.05\pm0.02$  mag in both bands. A very few images were obtained through thick clouds and were not used in our light curve analysis. Since the conditions were non-photometric, standard stars were not observed on either night. However, using the public release 2MASS data we determined a J and K' magnitude for a random bright star (RA=11:15:50, DEC=+42:55:20) within our field of view. Differential photometric results indicated that our two comparison stars did not vary by more than that expected due to photon statistics over the course of our observations. Therefore, we could use the bright 2MASS star to assign standard J and K' magnitudes to our comparison stars. In turn, this allowed us to transform our differential results for AR UMa into calibrated J and K' magnitudes. We found mean J and K' magnitudes for AR UMa on both nights of  $J=14.0\pm0.15$  and  $K'=13.2\pm0.15$ . The 2MASS survey also measured AR UMa itself and found it to have  $J=14.1$  and  $K'=13.3$ . These two measurements of J and K' for AR UMa are consistent within the uncertainties and within the 0.25 mag peak-to-peak variations in both J and K' light curves. Our resulting J and K' band light curves of AR UMa, phased

to the Schmidt et al. (1999) ephemeris, are presented in Figure 1.

### 3. Modeling the Light Curve of AR UMa

#### 3.1. Observational Evidence

The secondary star of AR UMa has been classified as an M6V $\pm$ 1 by Remillard et al. (1994), through analysis of an optical spectrum obtained in a low state. Using CV evolution models by Howell et al. (2000b), we can estimate the most likely mass for the secondary star in AR UMa. The secondary stars in CVs with orbital periods of less than two hours closely follow the lower main sequence mass-radius relation. Converting the determined mass ( $0.18 M_{\odot}$ ) into an assumed main sequence spectral type for the secondary star, we would expect it to be an M4V with  $T_{eff}=3,150$  K. We note here that the spectral analysis by Schmidt et al. (1999) gives a mass ratio of  $0.3\pm0.1$  which, when combined with their white dwarf mass ( $0.6 M_{\odot}$ ), also yields a secondary star mass of  $0.18\pm0.06 M_{\odot}$ .

Schmidt et al. (1996) found that a white dwarf ( $\log g = 8$ ) model having 98% of its projected area emitting at a temperature of  $T_{eff} \sim 15,000$  K, and only 2% of the surface covered by an accretion spot of  $T_{eff} \sim 35,000$  K, fit a combination of IUE and optical spectra. Schmidt et al. further determined that the observed flux results in a WD radius of  $8\times10^8$  cm, consistent with a  $0.6 M_{\odot}$  white dwarf. These same authors concluded that the white dwarf and the secondary star each contribute roughly one half of the flux in the V-band during the low state.

Combining the mean low state V magnitude and the mean I band magnitude from Remillard et al. (1994) with our mean J and K' magnitudes, we see that AR UMa has V-K'=3.3, I-K'=2.2, and J-K'=0.8. Within our errors, the infrared (I-K' and J-K') colors are consistent with an M4V secondary while the optical colors (V-I, V-J, or V-K'), however, are consistent with a K8V (Cox 2000; Glass 1999). Since a K8 star ( $0.60 M_{\odot}$ , appropriate for a CV with  $P_{orb}\sim 5$  h) would not fit into the Roche lobe of a 1.9 h binary, we view these colors as caused by contamination by the hotter white dwarf. Another possibility for the additional blue component may be the accretion region. Szkody et al. (1999) used X-ray and EUV data to show that the accretion region temperature is quite high, near 250,000 K, during high accretion states. This temperature must be taken as an upper limit since, as noted above, Schmidt et al. (1996) determined the accretion spot temperature to be substantially cooler only a few months after a transition to a low accretion state. This hot component might initially seem to be a likely candidate for the additional blue component we need, but with its extremely small size (even at its hottest), it provides no meaningful

flux contribution ( $<1\%$ ) to our light curves in either the infrared or in the optical. This supplies further evidence of the white dwarf contamination in the optical.

Light curves of magnetic cataclysmic variables, particularly those obtained during low states in the R or I visible bands or in the near infrared, are often observed to have a double-humped appearance with the cause of this shape generally assumed to be ellipsoidal variations due to the secondary star. Details of this claim are rarely presented; the light curve shape is left to attest to its cause simply by inference. Ellipsoidal variations should peak at orbital phase 0.25 and 0.75 (maximum projected area of the Roche lobe) and should have a cosine-like shape. Cyclotron emission radiated from near the accretion region can also provide increased light at nearly these same phases. Near the white dwarf magnetic poles, the magnetic field lines are approximately perpendicular to the surface and the location of the dynamically favored (active) pole is generally near binary phases 0.8-0.9. Thus, typical cyclotron beaming, strongest at  $90^\circ$  to the field lines (see Wickramasinghe and Ferrario 2000), will contribute increased system light preferentially centered near phases which are approximately coincident with the peak emission expected from ellipsoidal variations. For example, Gänsicke et al. (2000) show this to be the case at V for AM Herculis during a high state. Geometric factors such as the binary inclination, the accretion region co-latitude, and the location of the active magnetic pole, as well as physical properties such as  $B$  and  $\dot{M}$  all conspire to make the exact phasing and shape of the photometric signal caused by cyclotron beaming unique for any given polar. As we will see, even during polar low states, cyclotron beaming can provide a relatively strong photometric modulation, leading to a double-humped light curve similar in appearance to ellipsoidal variations.

Szkody et al. (1999) noted that the appearance of the AR UMa V band light curve changes significantly between high and low states, showing a single peaked sine-like structure centered near phase 0.4 when bright, and a double-humped structure suggestive of ellipsoidal variations when faint. We noted that the amplitude of the low state photometric humps seen at V (Szkody et al. 1999) was quite large and their flux peaked at orbital phases which were different from what was observed at I (Remillard et al. 1994; Schmidt et al. 1996) and in our infrared data. Ciardi et al. (2000) show that during a high state of HU Aqr the IR light curve is double humped but not well fit by ellipsoidal variations, their amplitude being too large and their shape being distinctively non-sinusoidal. However, low state IR photometry of this same star agrees with ellipsoidal models quite well (Ciardi et al. 1998). Recent IR spectral results for the polar ST LMi (Howell et al. 2000a) showed that during an extreme low state, the secondary star provides evidence for star-spot activity and the IR light curve does not appear to be double-humped at all.

We did not obtain simultaneous V band measurements of AR UMa which could be

used to confirm its accretion state during our IR observations. However, K. Honeycutt (private communication) has informed us that RoboScope observations provided relatively dense photometric monitoring of AR UMa during the interval of 26 January to 6 March 2000, and the star was consistently between  $V=16.6$  and  $V=16.8$  mag, firmly in the low state.

Given the possible confusion related to the presence or lack of ellipsoidal variations in polar light curves, particularly during low states, and the additional blue contribution seen in the colors of AR UMa, we decided to attempt detailed modeling of the low state light curves of AR UMa.

### 3.2. Model Setup

To model the light curves, we used WD98, the newest version of the Wilson-Devinney light curve program (Kallrath 1999; Wilson 1999). WD98 is an enhanced version of WD95 (Kallrath et al. 1998), updated with new features such as the addition of semi-transparent circumstellar clouds, a simple spectral line profile capability for fast-rotating stars, an option to work with either observed times or phases, and conversion of all the variables to double precision. Some of the relevant features of WD98 include: Kurucz atmosphere models for numerous wavelengths, a choice of three different limb darkening laws, proximity and eclipse effects, the option for hot or cold stellar spots, and several different modes of operation for various system geometries. The program has been fully described in papers by Wilson and Devinney (1971) and by Wilson (1979, 1990, 1993). A recent application of WD95 can be found in Milone et al. (2000).

Briefly, WD98 works as follows. It takes the photospheres of the stars and divides them up into a multitude of surface elements. The amount of light coming from each element is calculated based on the binary system input parameters. All of these surface elements are then summed together, based on the line-of-sight geometry, to create the final light curve.

There are a large number of input parameters needed to generate a model light curve for a complex binary system such as AR UMa. We discuss each of the most important of these parameters in the following subsections. We have made use of the best available literature system parameters and we list our wavelength independent input values to WD98 in Table 1. Units are shown where appropriate. We ran WD98 in a mode set up to produce a model for a semi-detached binary with the secondary star automatically filling its Roche lobe. We now discuss some of the input parameters in detail.

### 3.3. Limb Darkening

The most important parameter that affects both the shape and the amplitude of the ellipsoidal variations is limb darkening. WD98 allows you to choose from several different forms of limb darkening: linear, logarithmic, or square-root. The linear law,

$$I_{\lambda}(\mu) = I(1)(1 - x_{\lambda}(1 - \mu)),$$

was first investigated by Milne in 1921. In this equation,  $I_{\lambda}$  is the beam intensity at wavelength  $\lambda$ ,  $\mu$  is the cosine of the angle between the atmosphere normal and the beam direction, and  $x_{\lambda}$  is the limb darkening coefficient. As an alternative to this, KlingleSmith & Sobieski (1970) proposed the logarithmic law,

$$I_{\lambda}(\mu) = I(1)(1 - x_{\lambda}(1 - \mu) - y_{\lambda}\mu\ln(\mu)),$$

where  $y_{\lambda}$  is the non-linear limb-darkening coefficient. Díaz-Cordovés & Giménez (1992) introduced the square-root law,

$$I_{\lambda}(\mu) = I(1)(1 - x_{\lambda}(1 - \mu) - y_{\lambda}(1 - \sqrt{\mu})).$$

When fit to ATLAS atmosphere models, the logarithmic law appears to fit UV models the best, while the square-root law appears better at infrared wavelengths (Van Hamme 1993). Models run by Claret (1998) for very low mass, solar metallicity stars ( $2000 \text{ K} \leq T_{eff} \leq 4000 \text{ K}$ ) indicate that the square-root law best describes the intensity distribution in the infrared. We ran test models of stars with equal temperature and gravity, and found that the logarithmic and square-root laws produced nearly indistinguishable light curves. For the final models presented here, the square-root limb darkening law was adopted.

As shown by Alencar & Vaz (1999) the limb darkening coefficients of stars in close binaries can be effected by irradiation. Szkody et al. (1999) attribute the high state V band light curve shape in AR UMa to irradiation of the secondary by the accretion region on the white dwarf surface. There is no evidence for such irradiation during low states. In AR UMa, with a hot white dwarf primary and even hotter accretion region, it is important, however, to investigate whether irradiation has a perceivable effect on the limb darkening coefficients even during a low state. Due to the small size of the accretion spot and the low luminosity of the white dwarf, the models of Alencar & Vaz (1999) imply that the limb darkening coefficients used in our AR UMa models will not be significantly affected by irradiation during a low state, and thus we have used the normal, non-irradiated, coefficients. Note, we are not ignoring the reflection effect due to irradiation here, we are merely stating that irradiation does not affect the limb darkening coefficients of AR UMa.

### 3.4. Gravity Darkening

The second most important static parameter that affects the amplitude of the ellipsoidal variations is gravity darkening. Gravity darkening (a.k.a. brightening) deals with the localized temperature of a star’s surface. The functional form for gravity darkening,  $T_{eff} \propto g^\beta$ , is wavelength independent, and is not strongly affected by changes in either the mixing length or composition of the star. The amount of gravity darkening depends on how energy is transported through the star, and is thus correlated with the mass of the star. For low mass, convective stars,  $\beta=0.08$ , and for stars with radiative envelopes,  $\beta \sim 1$  (Lucy 1967). For the white dwarf primary in AR UMa, we have assumed no gravity darkening ( $\beta=0$ ). For the cool secondary stars used in our models, we have used a value of  $\beta=0.08$ .

### 3.5. Other input parameters

There are a variety of other input parameters with less freedom in their selection. For example, we must choose the values for the temperatures and monochromatic luminosities of the primary and secondary stars. The monochromatic luminosities of the 15,000 K white dwarf proposed by Schmidt et al. (1996), were calculated from a simple blackbody model. For the secondary stars, we calculated the corresponding luminosities using Bessell’s tabulation (Bessell 1991) of absolute magnitudes of cool, late type, main sequence stars. For models with an M4V secondary, we used a secondary temperature of  $T_{eff}=3,150$  K, and for models with an M6V secondary (as proposed by Remillard et al. 1994), we used a temperature of  $T_{eff}=2,800$  K.

In order to gauge what differences would occur between the two candidate secondary stars in AR UMa, we ran identical WD98 models for an M4V and an M6V star using the same inclination angle of  $70^\circ$ . This choice of  $i$  is not completely arbitrary as will be seen below. It can be seen in Figure 2 that an M6V secondary would play a small role in the production of ellipsoidal variations at V, even at this high inclination. Additionally, an M6V secondary star would not provide enough V flux to account for the 50% contribution that has been proposed by Schmidt et al. (1996). While the two models are similar at J and K’, we will see below that the I, J, and K’ modulations are indeed ellipsoidal variations and therefore require the earlier type secondary. Based on the work presented in Howell et al. (2000b), and our discussion here related to Figure 2, we have chosen to use a M4V secondary star in all of our following models.

The atmospheres of cool stars are fairly complicated and the details of their spectral energy distributions and any changes in such as a function of temperature, make for complex



modeling (cf., Allard et al. 1997). Stellar atmosphere codes have to take into account numerous atomic and molecular absorption features which affect the limb darkening coefficients. In order to accurately model the limb darkening effects of the secondary star in AR UMa, we used a Kurucz model for its atmosphere, the most complete atmosphere model available (Kurucz 1993; Kallrath & Milone 1999). Since the atmospheres of hot stars are much less complicated, particularly degenerate stars with thin atmospheres, we chose to model the white dwarf atmosphere as a blackbody.

Irradiation of the secondary star atmosphere in close binaries such as AR UMa can be very important. WD98 calculates reflection/re-radiation of irradiation based on the bolometric albedos of the two stars. The expected value for radiative envelopes like the white dwarf in AR UMa is unity. On the other hand, the bolometric albedo for the convective secondary star is expected to lie somewhere between 0.5 and 1, based on models run by Nordlund and Vaz (Nordlund & Vaz 1990; Vaz & Nordlund 1985). This value is dependent on the amount of convection in the star: the smaller the mixing length parameter,  $\alpha = l/H_p$ , the closer it is to a radiative atmosphere, and the higher the bolometric albedo. Based on the average of the albedos given in Table 3 of Nordlund & Vaz (1990) for grey atmosphere models with a 6,000 K star irradiating a 4,500 K star, we chose to model AR UMa’s secondary with a bolometric albedo of 0.676. The values published by Nordlund & Vaz cover only a few binary star scenarios. We have chosen the one that most closely resembles our system. Even though the system temperatures in Nordlund & Vaz are not the same as those in AR UMa, the scatter in the observed data is greater than the change in the light curves with albedos differing by  $\pm 0.1$ .

WD98 has the capability to handle spots (hot or cold) on the component stars. In order to make our model more realistic, we added a small, circular bright spot ( $R_{spot} = 0.05 R_{WD}$ ;  $T_{spot} \sim 250,000$  K) to our white dwarf. This spot represents the active magnetic accretion region near the south pole of the white dwarf, and was modeled using parameters determined by Schmidt et al. (1999) and Szkody et al. (1999). Although the models were run with the accretion spot included, as noted earlier, the hot spot did not have any significant effect on AR UMa’s light curves due to its small projected area. Ciardi et al. (1998), included a similar accretion region in their spectral energy distribution models of the polar HU Aqr and also found that the hot accretion region contributed essentially 0% to the flux in the visible and IR spectral regions.

Our AR UMa J and K’ band observations and their corresponding WD98 models for three possible values of the binary orbital inclination ( $50^\circ$ ,  $70^\circ$ , and  $90^\circ$ ), are presented in Figure 3. The points represent the data while the lines represent the models. We also ran WD98 models in the optical spectral region to compare with V band data from Szkody

et al. (1999) and maxima and minima I band data points taken from Remillard et al. (1994). The V and I band models (Figure 4) were run with the same wavelength independent input parameters as the infrared models, but with appropriate monochromatic luminosities, Kurucz model atmospheres, and limb darkening coefficients. Our choice to model three different inclinations was inspired by the desire to see what differences inclination makes at these band-passes, to span the range of possible system inclinations for AR UMa, and to understand how one might make use of such models to help determine system parameters.

#### 4. Results and Discussion

Examination of the  $50^\circ$  model in Figs 3 & 4 shows that the observed photometric amplitudes are not well matched by ellipsoidal variations alone. At  $50^\circ$ , an additional light source would be required in all bands. Increasing the inclination to  $70^\circ$ , slightly out of the range proposed by Schmidt et al. (1999), we find a good correlation with the observations except at V. The inclination can not be much higher as CVs with system inclinations larger than  $\sim 72^\circ$  will produce some observational evidence for an eclipse by the secondary star of either a part of the accretion stream, the white dwarf, or both. AR UMa shows no sign of such behavior. Forgetting the V band data for a moment, removal of the model fits from the observed data shows that the observed J and K' modulations are well fit by ellipsoidal variations alone (Figure 5). From Fig. 4, we see that this would also hold true for I band observations. Our results clearly favor a binary inclination for AR UMa of near  $70^\circ$ .

If we try to reconcile  $i=50^\circ$ , we note that the J and K' light curves would show a 0.15 mag flux excess peaking near phases 0.25 and 0.75. These phases are coincident with those times during which the observer would view the gas stream between the two stars at its maximum projected angle. Using an ad hoc gas stream model of rectangular dimensions and a uniform blackbody temperature of 6,500 K, we can only account for the 0.15 mag increase needed at J and K', if the emitting gas stream area was 50 times that of the white dwarf. This same model would have the gas stream producing 4 times the flux of the white dwarf at V. Given the nature of the low state spectral observations (cf. Schmidt et al. 1999), this simple gas stream model seems unable to account for the excess light needed if  $i=50^\circ$ . We could continue to modify our simplistic gas stream model by varying the temperature, emitting area, and even adding in a coupling region with some non-spherical shape, but the wisdom of Occam's razor<sup>1</sup> prevails.

---

<sup>1</sup>Occam's razor is "not to compound hypothetical features or mechanisms of a scenario beyond necessity" (*Entia non sunt multiplicanda praeter necessitatem*). However, William of Occam (1285-1349) is only known

For any value of  $i$ , it is clear that the V data can not be fit by ellipsoidal variations alone. In Figure 5, we see that the ellipsoidal variation subtracted V light curve shows significant positive residuals with peaks at orbital phases 0.15 and 0.67, not at 0.25 and 0.75. Thus, we must seek an independent source of these 0.1 mag photometric modulations.

We now explore cyclotron emission as a possible cause for the double-humped structure observed in the V light curve. Schmidt et al. (1999) used circular polarization measurements to determine that the magnetic longitude of the northern pole,  $\psi_N$ , was equal to  $90 \pm 7$  degrees, that is, at a right angle to the line of centers. Assuming diametrically opposed poles, the southern active pole would be located near  $\psi_S = 270^\circ$  or binary phase 0.75. Observations of AR UMa made during a high state in the EUV spectral region (Szkody et al. 1999; Belle et al. 2000) show that the peak emission occurs near orbital phase 0.92. Sirk & Howell (1998) modeled a number of similar EUV light curves for polars and found that in all cases, the value of  $\psi_{active}$  is coincident with the phase of maximum flux. Using the EUV results for AR UMa, we estimate  $\psi_S$  to be near longitude  $330^\circ$ . This apparent change in  $\psi_S$ , compared with  $270^\circ$  implied by Schmidt et al. (1999), is not as dramatic as it first appears, changing the physical location of the active region by very little <sup>2</sup>. If  $\psi_S = 330^\circ$  is correct (yielding  $\psi_N = 150^\circ$ ), then we would predict cyclotron emission to be a maximum near orbital phases 0.67 & 0.17. These are the phases of peak emission observed in our residual V band light curve (Figure 5).

However, the estimated field strength of 230 MG for AR UMa places the fundamental cyclotron harmonic near  $4660 \text{ \AA}$  (for non-relativistic cyclotron radiation; Ingham, Brecher & Wasserman 1976). With the fundamental and all higher harmonics (i.e., cyclotron humps) being blue-ward of the V band, it would seem unlikely that cyclotron radiation can provide the needed flux. Wickramasinghe & Ferrario (2000) show that for almost all polars, the field strength of the two poles differ by a ratio of 1.4-2, an effect assumed to be caused by a dipole offset from the white dwarf center by 10-30% of its radius. The active accreting pole, in all but one case, lies within  $\pm 45^\circ$  of the line of centers and in all cases the active pole is the weaker of the two. The strength of the magnetic field ( $B = 230 \text{ MG}$ ) in AR UMa was determined for the northern pole and not the active accreting southern pole, thus the latter might be of weaker strength.

---

to have written *Pluralitas non est ponenda sine necessitas*, “Plurality should not be posited without necessity” (Thorburn 1918). Notable newer versions of Occam’s razor are: *We are to admit no more causes of natural things than such as are both true and sufficient to explain their appearances* (Isaac Newton), *Everything should be as simple as possible, but no simpler* (Albert Einstein), and *Keep it simple!* (anonymous). The earliest quoted version of this razor is *Nature operates in the shortest way possible*, attributed to Aristotle.

<sup>2</sup> This is due to the fact that lines of longitude quickly become degenerate near a pole.

In order for our V band modulations to be caused by cyclotron emission, we would need the fundamental cyclotron harmonic ( $\nu_c$ ) to move red-ward to at least within the V band. Taking a red limit for  $\nu_c$  at 5500 Å, we require the magnetic field in AR UMa to be  $\lesssim 190$  MG. Recent UV spectroscopy of AR UMa (Gänsicke 2000) has revealed cyclotron humps and model fits estimate the magnetic field strength of the southern accreting pole to be 160 MG. At 160 MG, the (southern) accreting pole is the weaker of the two and the ratio of the pole strengths in AR UMa is 1.44, placing it in the typical range for polars. To account for the observed photometric amplitudes seen in V, the peak flux of the cyclotron emission would need to be  $1 \times 10^{-16}$  ergs s $^{-1}$  cm $^{-2}$  Å $^{-1}$  at 5500 Å. Our upper limit for the southern pole field strength and our flux estimate for the maximum needed cyclotron emission in V are both in agreement with the results provided by Gänsicke (2000).

In AR UMa, Schmidt et al. (1999) and Belle et al., (2000) show that the active magnetic pole is the southern, dynamically favored one, and due to the combination of the system inclination and the location of this pole on the white dwarf, it is never in direct view for an Earthly observer. If the pole is not seen directly, the high state EUV observations provide information on flux emitted from above the accretion region, not directly from the white dwarf surface. The peak EUV emission at phase 0.92 would then have to be interpreted as emanating from within the accretion column itself, some small distance above the magnetic pole. It is indeed possible that in this very high field system, the magnetic field close to the pole is not normal to the surface of the white dwarf and has a very complex structure. If true, the usual observational interpretations are invalid and without a direct view of the southern active pole, its true location may be hard to determine.

The observed low state photometric light curves are consistent with  $i=70^\circ$ ,  $B \lesssim 190$  MG, and  $\psi_S=330^\circ$  given that I, J, and K' modulations are nearly 100% ellipsoidal in nature and the V band modulations, centered at phases 0.15 and 0.67, are dominated by cyclotron emission. Our field strength of  $B \lesssim 190$  MG for the southern accreting pole is in agreement with the recent value of 160 MG found using model fits to cyclotron humps seen in UV spectra. While our data are not of sufficient quality or time sampling to extend or refine the above arguments, one result that does come from this work is that any simple interpretation of a polar light curve as solely due to ellipsoidal variations should be viewed with caution. Each polar will provide a unique array of physical and geometric characteristics to deal with.

The authors wish to thank Kent Honeycutt for providing us with the RoboScope data for AR UMa, and Paula Szkody for sending us the AR UMa V band data. David Ciardi, Paula Szkody and Gary Schmidt provided valuable discussions related to this work. Boris Gänsicke is thanked for providing his results prior to publication. DMG would like to thank Josef Kallrath and Bob Wilson for the use of WD98, as well as their help in running and

understanding the program. Comments from the anonymous referee were very useful and appreciated. This paper made use of the on-line 2MASS database. SBH acknowledges partial support of this work by NSF grant AST 9818770, NASA grant NAG5-8644, and an EUVE mini-grant. This research was also supported by a Grant-in- Aid of Research from the National Academy of Sciences, through Sigma Xi, The Scientific Research Society. DMG holds an American fellowship from the American Association of University Women Educational Foundation. KPNO/NOAO is operated by the Association of Universities for Research in Astronomy (AURA), Inc. under cooperative agreement with the National Science Foundation.

## REFERENCES

- Allard, F., Huaschildt, P., Alexander, D., & Starrfield, S., 1997, ARAA, 35, 137.
- Alencar, S.H.P., & Vaz, L.P.R., 1999, A&A Supp., 135, 555.
- Belle, K., Howell, S. B., & Sirk, M., 2000, PASP, submitted.
- Bessell, M.S., 1991, AJ, 101, 662.
- Ciardi, D., Howell, S. B., Hauschildt, P., & Allard, F., 1998, ApJ, 504, 450.
- Ciardi, D., Howell, S. B., & Sirk, M., 2000, in prep.
- Claret, A., 1998, A&A, 335, 647.
- Cox, A., 2000, “Allen’s Astrophysical Quantities”, Springer-Verlag, New York, Chps. 7, 15.
- Díaz-Cordovés, J., & Giménez, A., 1992, A&A, 259, 227.
- Gänsicke, B., 2000, Private Communication.
- Gänsicke, B., Fischer, A., Silvotti, R., & de Martino, D., 2000, A&A, submitted.
- Glass, I., 1999, “Handbook of Infrared Astronomy”, Cambridge University Press, Cambridge, UK, Chp. 3.
- Howell, S. B., Ciardi, D., Dhillon, V., & Skidmore, W., 2000a, ApJ, 530, 904.
- Howell, S.B., Nelson, L.A., & Rappaport, S., 2000b, ApJ, in press. (astro-ph/0005435)
- Howell, S. B., Mitchell, K. J., & Warnock, A., 1988, AJ, 95, 247.
- Ingham, W. H., Brecher, K., & Wasserman, I., 1976, ApJ, 207, 518.
- Joyce, R., 1999, IRIM Users Manual, <http://www.noao.edu/kpno/manuals/irim/>.
- Kallrath, J., 1999, Private Communication.

- Kallrath, J., Milone, E.F., 1999, *Eclipsing Binary Stars: Modeling and Analysis*, pp 220-221, Springer, New York.
- Kallrath, J., Milone, E.F., Terrell, D., & Young, A.T., 1998, *ApJ*, 508, 308.
- Klinglesmith, D.A., & Sobieski, S., 1970, *AJ*, 75, 175.
- Kurucz, R.L., 1993, *New Atmospheres for Modeling Binaries and Disks*, in E.F. Milone (Ed.), *Light Curve Modeling of Eclipsing Binary Stars*, pp. 93-102, Springer, New York.
- Lucy, L.B., 1967, *Zeitschr für Astrophys*, 65, 89.
- Milne, E.A., 1921, *MNRAS*, 81, 361.
- Milone, E.F., Schiller, S.J., Munari, U., & Kallrath, J., 2000, *ApJ*, 199, 1405.
- Nordlund, Å., & Vaz, L.P.R., 1990, *A&A*, 228, 231.
- Remillard, R.A., Schachter, J.F., Silber, A.D., & Slane, P., 1994, *ApJ*, 426, 288.
- Rusell, H. N., 1945, *ApJ*, 102, 1.
- Schmidt, G.D., Szkody, P., Smith, P.S., Silber, A., Tovmassian, G., Hoard, D.W., Gänsicke, B.T., & De Martino, D., 1996, *ApJ*, 473, 483.
- Schmidt, G.D., Hoard, D.W., Szkody, P., Melia, F., Honeycutt, R.K., & Wagner, R.M., 1999, *ApJ*, 525, 407.
- Sirk, M., & Howell, S. B., 1998, *ApJ*, 506, 824.
- Szkody, P., Vennes, S., Schmidt, G.D., Wagner, R.M., Fried, R., Shafter, A.W., & Fierce, E., 1999, *ApJ*, 520, 841.
- Thorburn, W. M., 1918, *Mind*, 27, 345.
- Vaz, L.P.R., & Nordlund, Å., 1985, *A&A*, 147, 281.
- Wickramasinghe, D., & Ferrario, L., 2000, *PASP*, 112, 873.
- Wilson, R.E., 1979, *ApJ*, 234, 1054.
- Wilson, R.E., 1990, *ApJ*, 356, 613.
- Wilson, R.E., 1993, in *New Frontiers in Binary Star Research*, ed K.C. Leung and I.S. Nha, A.S.P. Conf. Ser., 38, 91.
- Wilson, R.E., 1998, in *Reference Manual to the Wilson-Devinney Program, Computing Binary Star Observables*, Version 1998 (Gainsville, FL: Univ. Florida).
- Wilson, R.E., 1999, Private Communication.
- Wilson, R.E., & Devinney, E.J., 1971, *ApJ*, 166, 605.

Table 1. Wavelength Independent WD98 Input Parameters for AR UMa

Parameter	Value
Orbital Period <sup>a</sup> (days)	0.08050075
Ephemeris <sup>a</sup> (HJD phase 0.0)	2450470.4309
Semi-major axis ( $R_{\odot}$ )	0.72
Orbital eccentricity	0.0
Temperature of White Dwarf <sup>a</sup> (K)	15,000
Temperature of M4V Secondary (K)	3,150
Mass ratio ( $M_2/M_1$ )	0.3
Atmosphere model (WD)	blackbody
Atmosphere model ( $M_2$ )	Kurucz
Limb darkening Law	Square-root
Gravity darkening exponent (WD)	$\beta=0.00$
Gravity darkening exponent ( $M_2$ )	$\beta=0.08$
Bolometric Albedo (WD)	1.000
Bolometric Albedo ( $M_2$ )	0.676

<sup>a</sup>From Schmidt et al., 1999

### Figure Captions

Figure 1. AR UMa J band (top panel) and K' band (bottom panel) light curves. The data were obtained on 2000 February 13 and 14, with IRIM on the KPNO 2.1-m telescope. Here and throughout this paper we phase our heliocentric corrected data to the Schmidt et al. (1999) ephemeris.

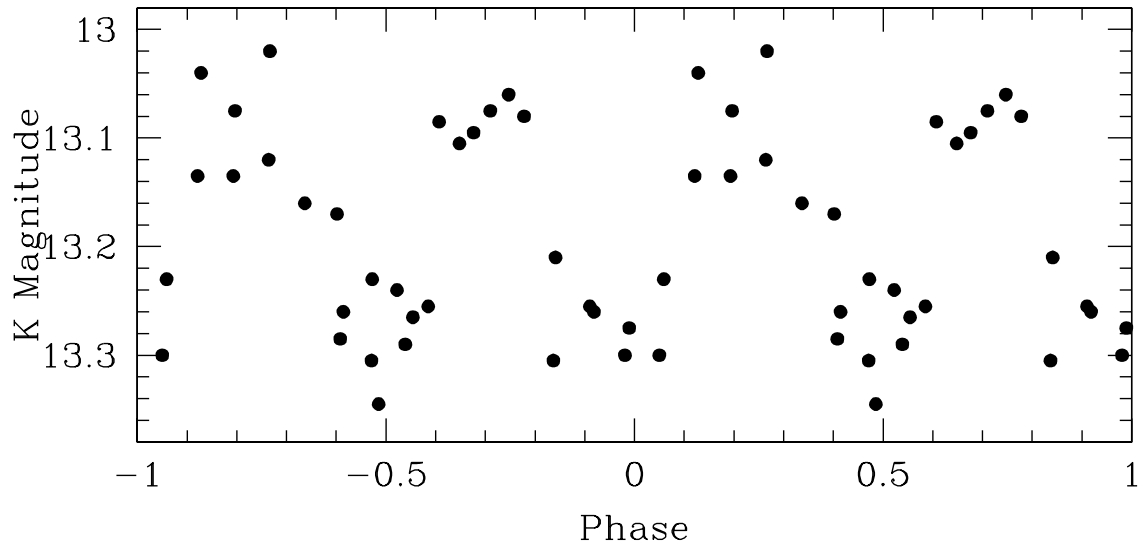
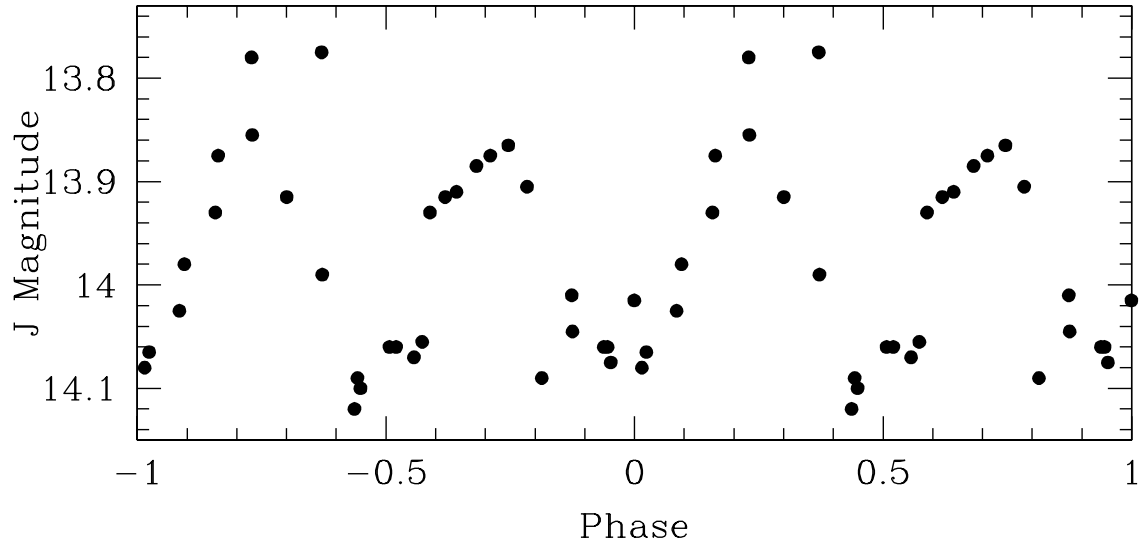
Figure 2. AR UMa V band (V-C; Szkody et al., 1999, Figure 1) & I band (Remillard et al., 1994, Figure 7) maxima and minima data (points) are shown in the top panel. Our J & K' band data (points) are shown in the bottom panel. The lines represent identical WD98 models for an M4V secondary star (solid line) and an M6V secondary star (dotted line), both for a binary inclination of  $70^\circ$ . The M4V and M6V models are similar at K' but clearly differ at the other wavelengths.

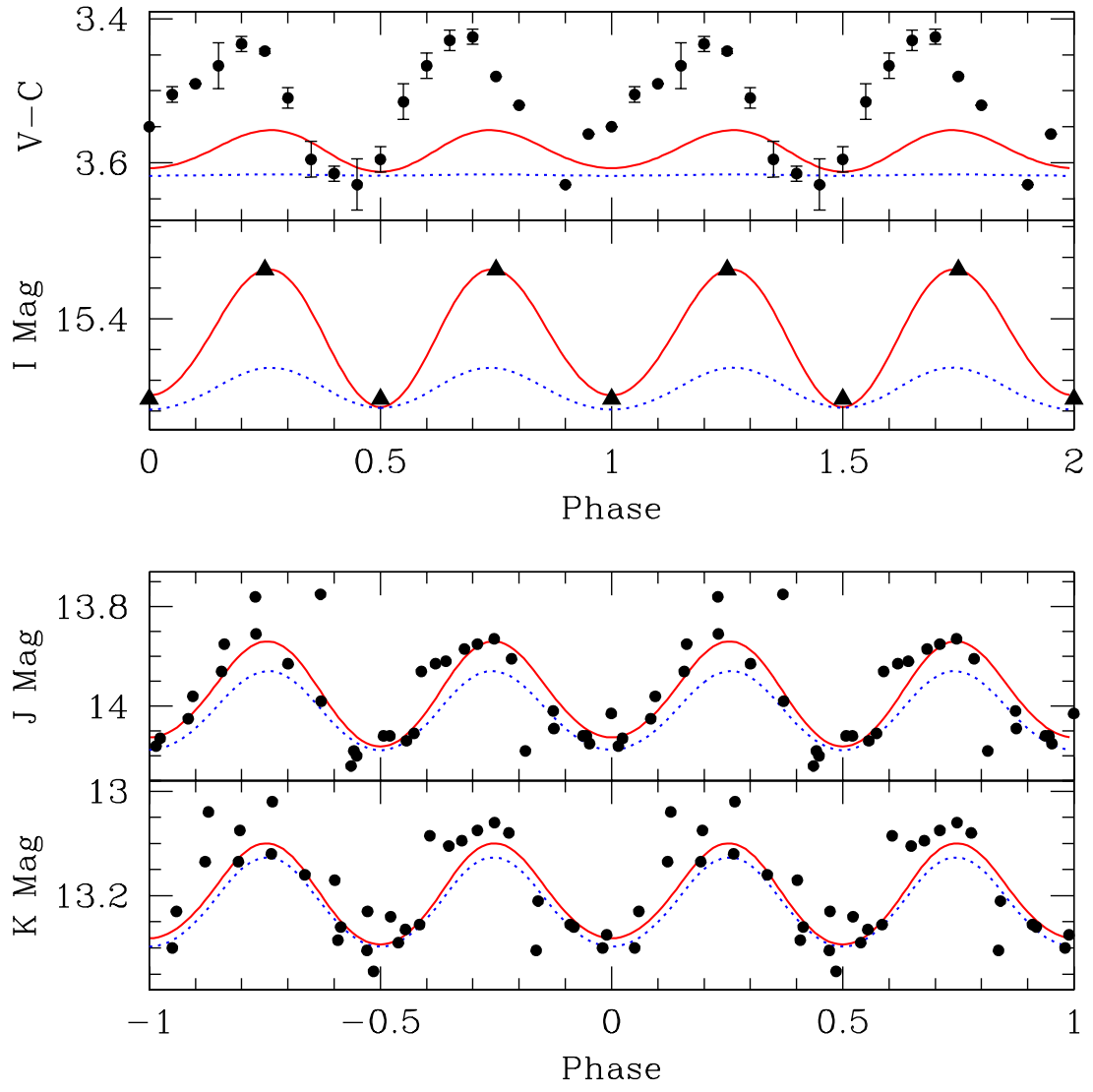
Figure 3. AR UMa J band (top panel) and K' band (bottom panel) data (points) from Figure 1, and three WD98 models. The models were run with the input parameters listed in Table 1 for orbital inclination angles of:  $50^\circ$  (dotted line),  $70^\circ$  (solid line), and  $90^\circ$  (dashed line).

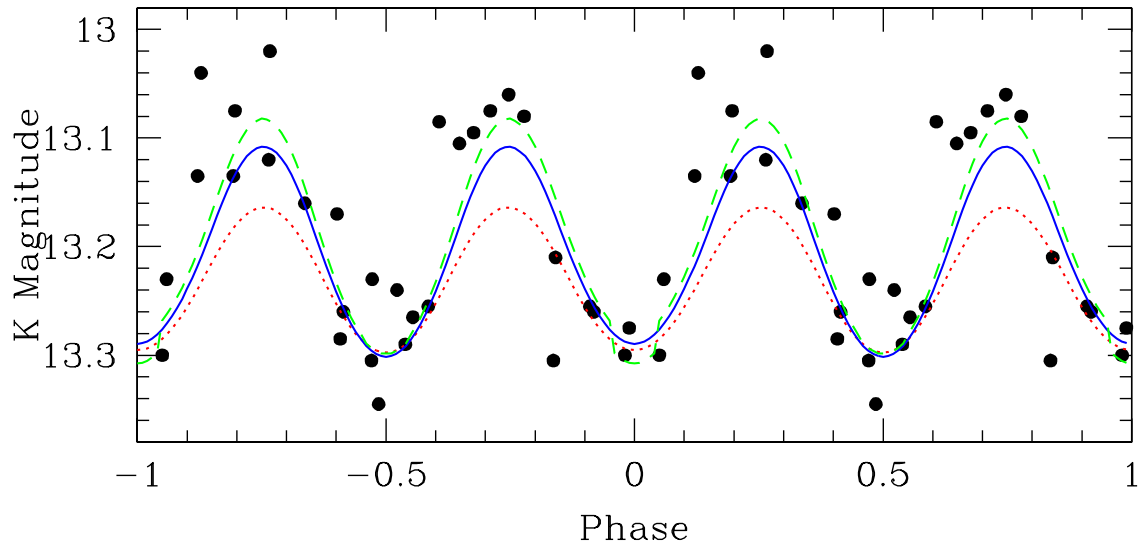
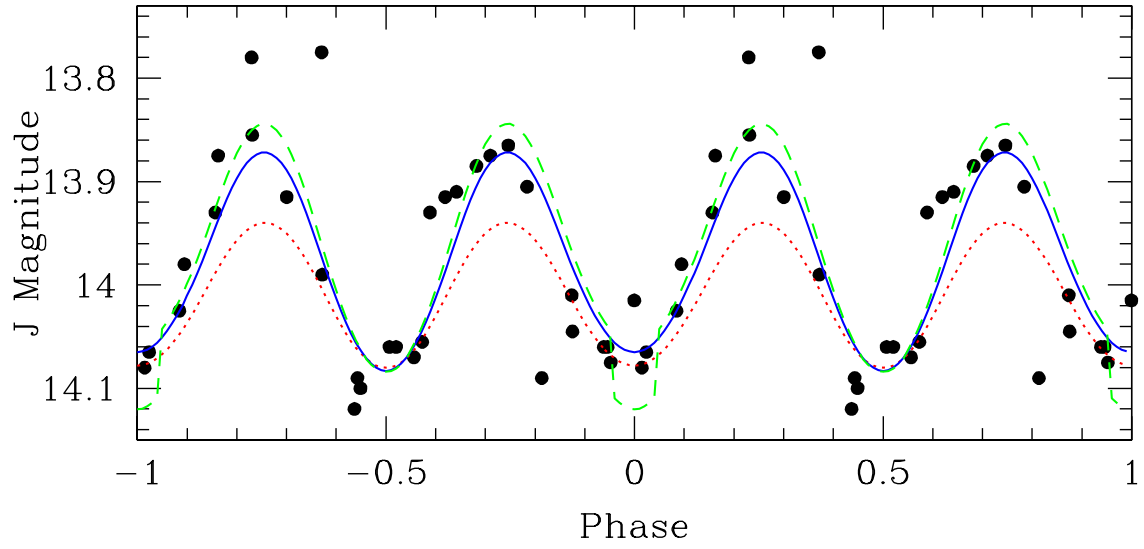
Figure 4. (Top panel) AR UMa V band data (points) from Figure 1 of Szkody et al. (1999). (Bottom Panel) Maximum and minimum I band data points taken from Figure 7 of Remillard et al. (1994). The lines represent WD98 models for the same three orbital inclinations as in Figure 3 ( $50^\circ$ -dotted line,  $70^\circ$ -solid line, and  $90^\circ$ -dashed line). In this case, the  $70^\circ$  model fits the I band data very well, but none of the models provide an adequate fit at V.

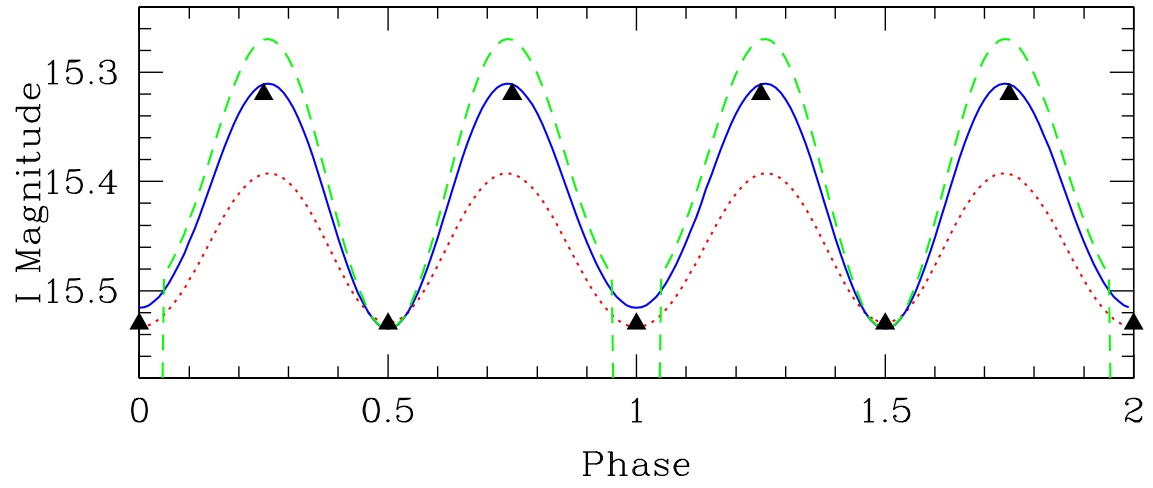
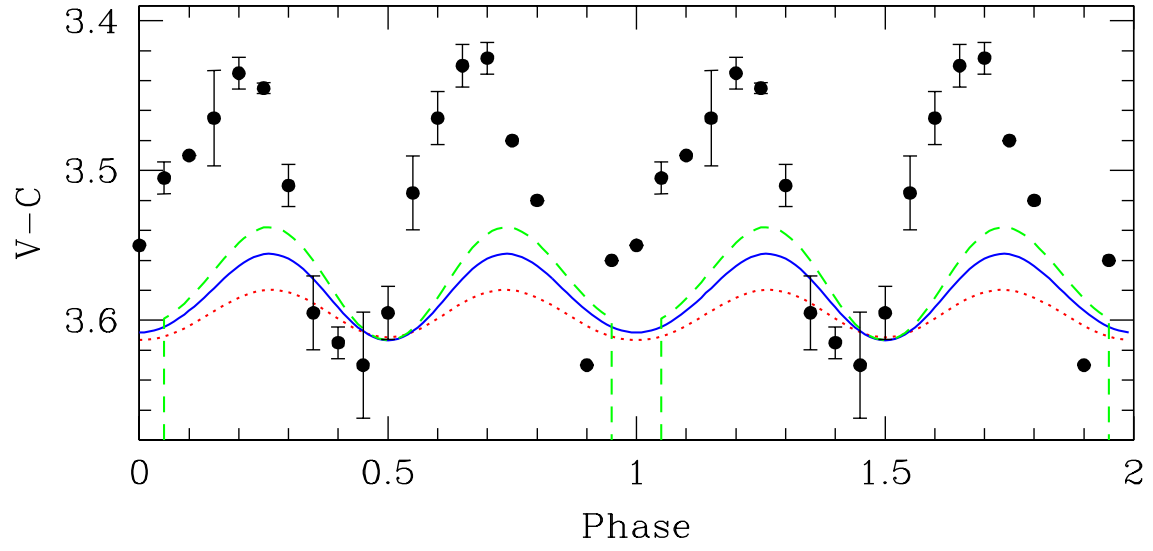
Figure 5. Differences (Observed AR UMa Data - Model) for the Szkody et al. (1999) V band data (top panel), our J band data (middle panel), and our K' band data (bottom panel). The differences are plotted for the  $70^\circ$  model and contain essentially no significant residuals at J and K'. However, the V data present a double-humped light curve of amplitude 0.1 mag with peaks at phases 0.15 and 0.67. The V band modulation is almost entirely due to cyclotron beaming.

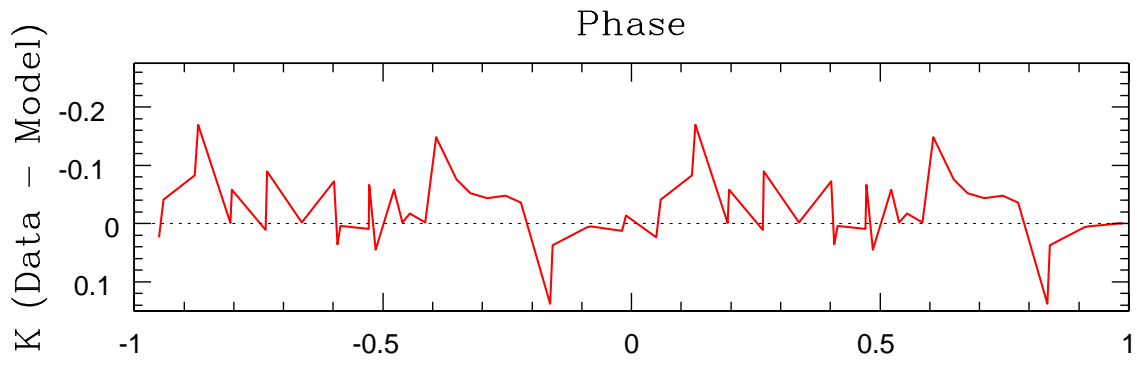
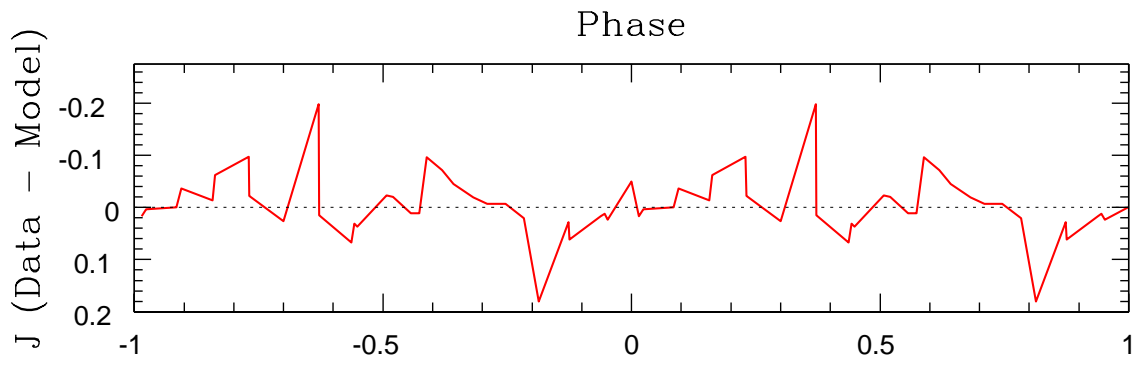
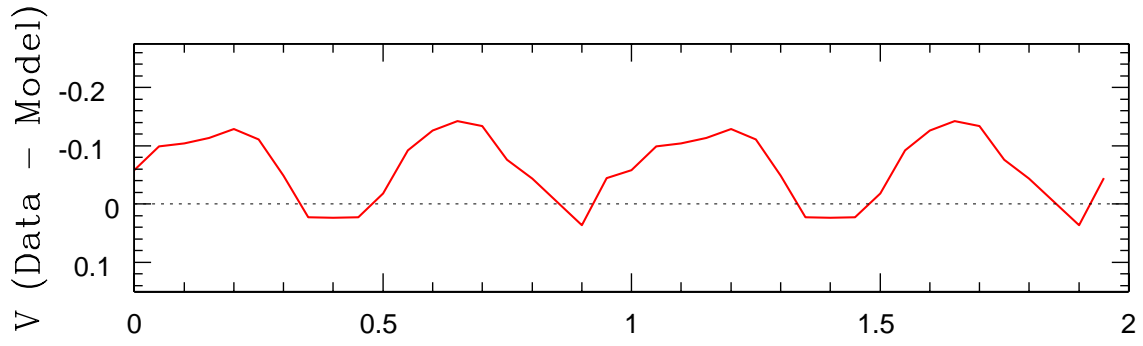












Phase